

*Journal of Organometallic Chemistry*, 149 (1978) 219-229  
© Elsevier Sequoia S.A., Lausanne — Printed in The Netherlands

The Molecular Structure of High- and Low-spin 1,1'-Dimethyl-  
manganocene Determined by Gas Phase Electron Diffraction

ARNE ALMENNINGEN, ARNE HAALAND and SVEIN SAMDAL

Department of Chemistry, The University of Oslo, Blindern,  
Oslo 3 (Norway)

(Received January 17th, 1978)

Summary

The electron diffraction pattern of 1,1'-dimethyl-  
manganocene has been recorded from  $s = 3.00$  to  $42.00 \text{ \AA}^{-1}$ .  
The gas is found to contain two geometrically distinct  
species. The most abundant species, mole fraction  $x = 0.62(4)$ ,  
has a Mn-C bond distance  $R(\text{Mn-C}) = 2.433(8) \text{ \AA}$  and vibrational  
amplitude  $u(\text{Mn-C}) = 0.111(8) \text{ \AA}$ . By comparison with the structure  
of the essentially high-spin complex  $(\text{C}_5\text{H}_5)_2 \text{Mn}$  where  $R(\text{Mn-C}) =$   
 $2.38 \text{ \AA}$ , it is concluded that the most abundant species is in the  
high-spin,  ${}^6\text{A}_{1g}$ , state. The less abundant species,  $x = 0.38(4)$ ,  
has an Mn-C bond distance  $R(\text{Mn-C}) = 2.144(12) \text{ \AA}$  and vibrational  
amplitude  $u(\text{Mn-C}) = 0.160(16) \text{ \AA}$ . This species is assumed  
to be in a low-spin,  ${}^2\text{E}_{2g}$ , state. The large Mn-C vibrational  
amplitude of the low-spin species is consistent with the  
existence of a dynamic Jahn-Teller effect involving the ring  
tilting modes.

---

## Introduction

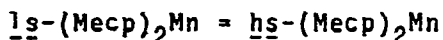
The metallocenes of the first row transition elements from vanadium to nickel,  $\text{Cp}_2\text{M}$ ,  $\text{Cp}$  = cyclopentadienyl,  $\text{M} = \text{V}, \text{Cr}, \text{Mn}, \text{Fe}, \text{Co}$  and  $\text{Ni}$ , have all been investigated by gas phase electron diffraction [1-7]. The M-C bond distances found are listed below with the electronic configurations of the molecules in the gas phase as determined by photoelectron spectroscopy by Evans *et al.* [8,9]:

Compound	R(M-C)/Å	Electron configuration	n
$\text{Cp}_2\text{Fe}$	2.064(3)	$^1\text{A}_{1g} (\underline{a}_{1g}^2, \underline{e}_{2g}^4)$	0
$\text{Cp}_2\text{Co}$	2.119(3)	$^2\text{E}_{1g} (\underline{a}_{1g}^2, \underline{e}_{2g}^4, \underline{e}_{1g}^1)$	1
$\text{Cp}_2\text{Cr}$	2.169(4)	$^3\text{E}_{2g} (\underline{a}_{1g}^1, \underline{e}_{2g}^3)$	2
$\text{Cp}_2\text{Ni}$	2.196(4)	$^3\text{A}_{2g} (\underline{a}_{1g}^2, \underline{e}_{2g}^4, \underline{e}_{1g}^2)$	2
$\text{Cp}_2\text{V}$	2.280(5)	$^4\text{A}_{2g} (\underline{a}_{1g}^1, \underline{e}_{2g}^2)$	3
$\text{Cp}_2\text{Mn}$	2.383(3)	$^6\text{A}_{1g} (\underline{a}_{1g}^1, \underline{e}_{2g}^2, \underline{e}_{1g}^2)$	5

If one assumes the  $\underline{a}_{1g}$  and  $\underline{e}_{2g}$  molecular orbitals to be bonding between the metal atom and the rings and the  $\underline{e}_{1g}$  orbital to be antibonding, one can define the electron imbalance of each complex,  $n$ , as the number of electrons in the  $\underline{e}_{1g}$  orbital plus the number of vacancies in the  $\underline{a}_{1g}$  and  $\underline{e}_{2g}$  orbitals [6]. The M-C bond distances are then found to increase monotonically with  $n$  from 2.06 Å in  $\text{Cp}_2\text{Fe}$  ( $n = 0$ ) to 2.38 Å in  $\text{Cp}_2\text{Mn}$  ( $n = 5$ ).

The photoelectron spectrum of  $\text{Cp}_2\text{Mn}$  shows that the compound is essentially high-spin ( $^6\text{A}_{1g}$ ) in the gas phase near room temperature. Only one "exceedingly weak" line indicated the presence of small amounts of low spin species [9]. Gaseous 1,1'-dimethylcyclopentadienylmanganese,  $(\text{Mecp})_2\text{Mn}$ , on the other hand, was found to consist of high-spin ( $^6\text{A}_{1g}$ ) and low-spin species in comparable amounts. Low temperature ESR studies by

Rettig and Ammeter and their coworkers [10,11] led to the identification of the low-spin species as  ${}^2E_{2g}(a_{1g}^2, e_{2g}^3)$ . Rettig and coworkers also studied the equilibrium



( $\underline{l_s}$  = low-spin,  $\underline{h_s}$  = high spin) in toluene over the temperature range -59 to 98 °C and determined the enthalpy and entropy of the reaction:  $\Delta H^\circ = 7.5 \pm 0.4 \text{ kJ mol}^{-1}$  and  $\Delta S^\circ = 24.3 \pm 2.5 \text{ J K}^{-1} \text{ mol}^{-1}$  [10].

Low spin,  ${}^2E_{2g}, (\text{Mecp})_2\text{Mn}$  has an electron imbalance equal to one and is therefore expected to have a M-C bond distance similar to  $\text{Cp}_2\text{Co}$  and considerably shorter than the bond distance found in the essentially high-spin complex  $\text{Cp}_2\text{Mn}$ . In order to test this hypothesis we decided to study  $(\text{Mecp})_2\text{Mn}$  by means of gas phase electron diffraction.

#### Experimental and data reduction

The sample of  $(\text{Mecp})_2\text{Mn}$  was a gift from Dr. M.L.H.Green, University of Oxford, and had been synthesized as described in reference [12]. It was purified by vacuum distillation at 90° before use. The electron scattering pattern was recorded on the Oslo electron diffraction unit [13] with a nozzle temperature of about 100 °C. Exposures were made with nozzle-to-photographic plate distances of about 48, 30 and 20 cm. The optical densities of four plates from the first set, six from the second, and four plates from the third were processed using the programs described by Andersen et al. / <sup>[14]</sup> The average modified molecular intensity values were calculated for each set and covered the s-ranges 3 to 19, 5 to 30, and 12 to 42 Å<sup>-1</sup> respectively. Finally these average curves were scaled and connected. The resulting modified molecular intensity points are shown in Fig. 1.

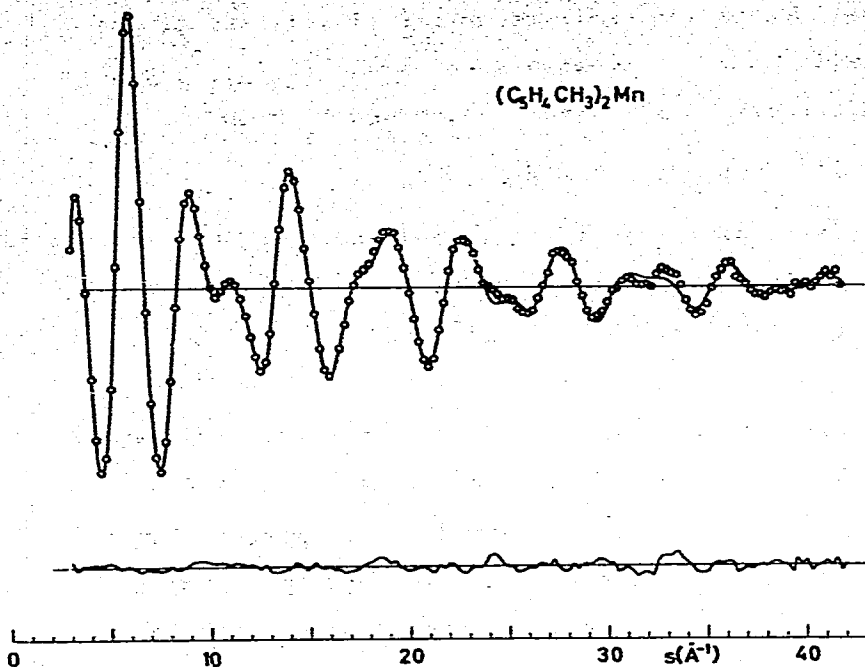


Fig. 1. Above:  $\circ$ : experimental modified molecular intensity points for  $(\text{Mecp})_2\text{Mn}$  from  $s = 3.00$  to  $42.00 \text{ \AA}^{-1}$ . Below  $s = 10.00 \text{ \AA}^{-1}$  only every second point is shown. Full line: Theoretical intensity curve calculated for best models. Below: Difference curve.

### Choice of model and structure refinement

A molecular model of  $(\text{Mecp})_2\text{Mn}$  is shown in Fig. 2.

It was assumed that:

- i) The parent metallocene,  $\text{Cp}_2\text{Mn}$ , has effective  $\underline{D}_{5h}$  or  $\underline{D}_{5d}$  symmetry in both the  ${}^6\text{A}_{1g}$  and  ${}^2\text{E}_{2g}$  states.

Our previous investigation of  $\text{Cp}_2\text{Mn}$ , which is essentially high-spin, has shown that the electron diffraction data are consistent with models of  $\underline{D}_{5h}$  and  $\underline{D}_{5d}$  symmetry with a very low barrier to rotation of the ligand rings. Low-spin  $\text{Cp}_2\text{Mn}$  has an orbitally degenerate ground state and suffers from a dynamic Jahn-Teller distortion involving the ring tilting

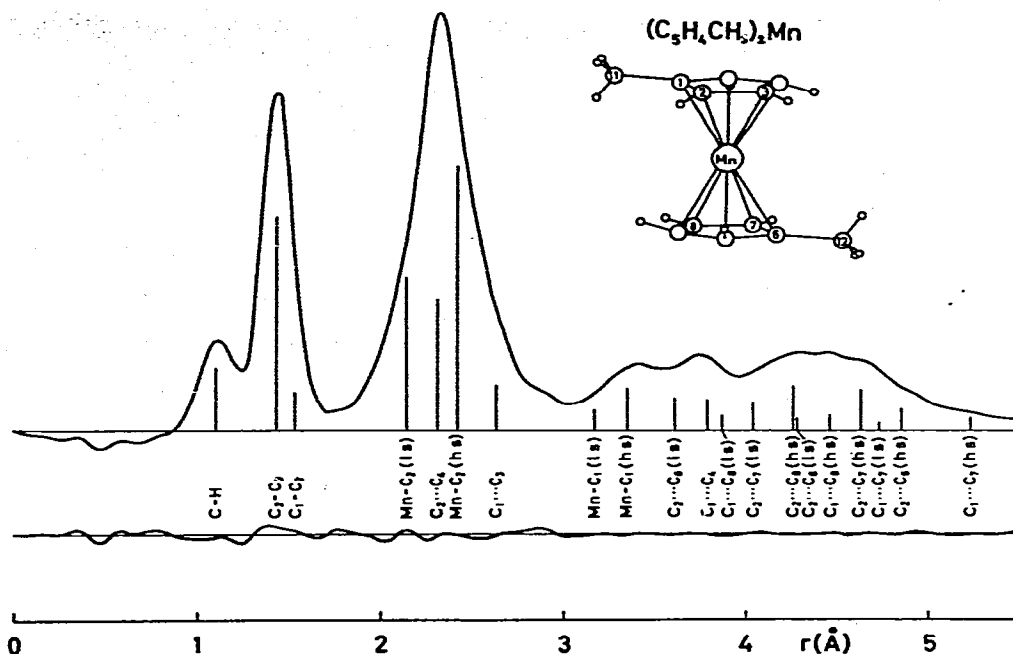


Fig. 2. Upper curve: experimental radial distribution curve for  $(Mecp)_2Mn$ . Lower curve: difference between the experimental curve and a theoretical radial distribution curve calculated for best models. Artificial damping constant  $k = 0.0013 \text{ \AA}^2$ .

modes [15]. However, previous investigations of  $Cp_2Cr$  [1] and  $Cp_2Co$  [6] which also have orbitally degenerate ground states, showed that average models of  $D_{5h}$  and  $D_{5d}$  symmetry could be brought into good agreement with the electron diffraction data.

Models for high- and low-spin  $(Mecp)_2Mn$  were constructed from the models of the parent metallocenes by removing a H atom on each ring and replacing it with a methyl group at a different  $C(Cp)-C(Me)$  bond distance and with a different angle between the bond and the plane of the  $C_5$  ring. It was assumed that:

- ii) Substitution of a H atom by a Me group leaves the geometry of the ring otherwise unchanged.
- iii) Each Me group has  $C_{3v}$  symmetry with the threefold axis coinciding with the  $C(Cp)-C(Me)$  bond. The angle of

rotation of the Me group about the C-C bonds is as shown in Fig. 2.

- iv) The structures of the ligands in high- and low-spin complexes are equal.

The structure of the ligands is then determined by seven independent parameters, e. g. the C(Cp)-H, C(Me)-H, C(Cp)-C(Cp) and C(Cp)-C(Me) bond distances, the valence angle  $\angle$ C(Cp)-C(Me)-H, and finally the angles between the C(Cp)-H and C(Cp)-C(Me) bonds and the C<sub>5</sub> plane of the ligand rings. These angles are denoted by  $\angle$ C<sub>5</sub>, H and  $\angle$ C<sub>5</sub>, C respectively and were defined as positive when the bonds are bent towards the metal atom. The  $\angle$ C-C-H valence angle could not be refined and was fixed at 109.5°.

The structure of  $\underline{h}_5$ -(Mecp)<sub>2</sub>Mn is determined by the six (remaining) ligand parameters plus a Mn-C(Cp) bond distance and a dihedral angle  $\phi$  describing the relative orientation of the two Mecp ligands. This angle was defined as zero when the rings are eclipsed and the Me groups syn. The structure of  $\underline{l}_5$ -(Mecp)<sub>2</sub>Mn is determined by the same six ligand parameters plus another Mn-C(Cp) bond distance and dihedral angle,  $\phi'$ .

The electron scattering pattern contains very little information about the dihedral angles  $\phi$  and  $\phi'$ : Of the 36 distances between C atoms in different ligand rings, only one, C(Me)---C'(Me) depends on the value of  $\phi$ . It was therefore assumed that  $\phi' = \phi$ , and least-squares refinements were carried out for a series of values of  $\phi$  ranging from 0 to 180°.

The molecular structures of  $\underline{h}_5$ - and  $\underline{l}_5$ -(Mecp)<sub>2</sub>Mn and their mole fractions as well as 14 of the most important root mean square vibrational amplitudes,  $\underline{u}$ , were refined by least-squares calculations on the connected intensity curve with a diagonal weight matrix and under the constraints of

geometrically consistent  $r_a$  structures and  $x_{\text{HS}} + x_{\text{LS}} = 1$ . The program used has been written by H.M. Seip. Theoretical modified molecular intensity curves were calculated from eq. 11 in reference [14].

It was found that satisfactory agreement between experimental and calculated intensities could be obtained for all values of the dihedral angle  $\phi$ . In Table 1 we list the parameter values obtained with  $\phi = 180^\circ$  since this value gave a slightly better fit than the others. The estimated standard deviations in the Table have been obtained from those calculated by the program after multiplication by a factor of 2.0 to take into account the additional uncertainty introduced by correlation in the experimental intensity data [16] and the assumptions outlined above, and expanded to take into account an estimated uncertainty of 0.1 % in the electron wavelength. Refinements with values of  $\phi$  different from  $180^\circ$  converged to parameter values that differed from those in the Table by less than 1.5 estimated standard deviation.

A modified molecular intensity curve calculated for the best model is shown in Fig. 1. An experimental radial distribution curve and the difference between this curve and one calculated for the best model is shown in Fig. 2.

### Discussion

In agreement with the photoelectron spectrum, it is found that gaseous  $(\text{Mecp})_2\text{Mn}$  at about  $100^\circ\text{C}$  contains two geometrically distinct species, one with  $\text{Mn-C}(\text{Cp}) = 2.433(8)$  Å, the other with  $\text{Mn-C}(\text{Cp}) = 2.144(12)$  Å. By comparison with the essentially high-spin complex  $\text{Cp}_2\text{Mn}$ ,  $\text{Mn-C} = 2.38$  Å, we conclude that the species with the larger Mn-C bond distance is in a high-spin,  ${}^6A_{1g}$ , state, while the species with the shorter

Table 1. Bond distances, valence angles, and root mean square vibrational amplitudes ( $\bar{u}$ ) of high spin and low spin  $\text{Mecp}_2\text{Mn}$ . (Estimated standard deviations in parenthesis)<sup>a</sup>

	R/A	$\bar{u}$ /A		R/A	$\bar{u}$ /A
<u>High spin</u>			<u>Ligand parameters</u>		
Mn-C(Cp)	2.433(8)	0.111(8)	C(Cp)-H	1.094(6) <sup>c</sup>	0.083(10) <sup>d</sup>
Mn---C(Me)	3.36(7)	0.16(5)	C(Me)-H	1.104(6) <sup>c</sup>	0.083(10) <sup>d</sup>
C <sub>1</sub> ---C <sub>8</sub>	4.28(2)	0.19(6)	C(Cp)-C(Cp)	1.427(2)	0.050(2) <sup>e</sup>
C <sub>1</sub> ---C <sub>7</sub>	4.65(2)	0.16(4)	C(Cp)-C(Me)	1.527(10)	0.056(2) <sup>e</sup>
C <sub>1</sub> ---C <sub>6</sub>	4.87(2)	0.43(25)	C <sub>1</sub> ---C <sub>3</sub>	2.309(2)	0.055(2)
$\bar{x}_{\text{hs}}$	0.62(4)		C <sub>2</sub> ---C <sub>11</sub>	2.630(8)	0.14(6)
			C <sub>3</sub> ---C <sub>11</sub>	3.787(10)	0.08(2)
			$\angle$ C-C-H	109.5 <sup>o</sup> <sup>b</sup>	
			$\angle$ C <sub>5</sub> ,H	-14(8) <sup>o</sup>	
			$\angle$ C <sub>5</sub> ,C	-6(4) <sup>o</sup>	
<u>Low spin</u>					
Mn-C(Cp)	2.144(12)	0.160(16)			
Mn---C(Me)	3.18(6)	0.20(10)			
C <sub>1</sub> ---C <sub>8</sub>	3.61(3)	0.11(4)			
C <sub>1</sub> ---C <sub>7</sub>	4.04(3)	0.26(10)			
C <sub>1</sub> ---C <sub>6</sub>	4.29(3)	0.40 <sup>b</sup>			
$\bar{x}_{\text{ls}}$	0.38(4)				

<sup>a</sup> For numbering of the atoms consult Fig. 2. The distances are given as  $r_a$ . The angles have not been corrected for shrinkage.

<sup>b</sup> Assumed value. <sup>c</sup> These bond distances were assumed to differ by 0.01 Å. <sup>d</sup> These amplitudes were assumed equal. <sup>e</sup> These amplitudes were assumed to differ by 0.006 Å.



Mn-C bond distance is in the low-spin,  ${}^2E_{2g}$ , state. The mole fractions of high- and low-spin species in the gas phase at about 100 °C,  $x_{h_s} = 0.62(4)$  and  $x_{l_s} = 0.38(4)$  are then in good agreement with the mole fractions found in toluene solution at 98 °C,  $x_{h_s} = 0.605$  and  $x_{l_s} = 0.395$  [10]. INDO self consistent field molecular orbital calculations on  $Cp_2Mn$  by Clack yielded equilibrium Mn-C bond distances equal to 2.07 Å for the  ${}^2E_{2g}$  state and 2.16 Å for the  ${}^6A_{1g}$  state [17], and are thus in qualitative agreement with experiment.

If the estimated standard deviations are taken at their face value, the Mn-C bond distance in  $h_s-(Mecp)_2Mn$ , 2.433(8) Å, would appear to be significantly longer than in  $h_s-Cp_2Mn$ , 2.383(3) Å. The structure determination in reference [2] was however carried out under the assumption that  $Cp_2Mn$  is 100 % high-spin. The photoelectron spectrum [9] shows, however, that a small amount of low-spin species probably must have been present in the gas jet during the electron diffraction experiment. New least squares refinements of  $Cp_2Mn$  where this possibility is taken into account, has been initiated and the results will be published later.

As expected the M-C bond distance of  $l_s-(Mecp)_2Mn$ , 2.144(12) Å, is quite similar to that of  $Cp_2Co$ , 2.119(4) Å: Both these complexes have an electron imbalance equal to one. The large Mn-C vibrational amplitude of  $l_s-(Mecp)_2Mn$ , 0.160(16) Å, is in good agreement with the existence of a dynamic Jahn-Teller effect involving the ring tilting modes as found by Ammeter and coworkers [15].

Ammeter and coworkers have also measured the ESR spectra of  $Cp_2Mn$  doped into polycrystalline samples of  $Cp_2Mg$ ,  $Cp_2Fe$  and  $Cp_2Ru$  [11]. The spectra at 4 K show the ground state to be  ${}^6A_{1g}$  in  $Cp_2Mg$ , but  ${}^2E_{2g}$  in  $FeCp_2$  and  $RuCp_2$ . Clearly the lattice of  $Cp_2Mg$  (Mg-C = 2.34 Å [18,19]) can accommodate the large

high-spin species of  $\text{Cp}_2\text{Mn}$ , while the lattices of  $\text{Cp}_2\text{Fe}$  ( $\text{Fe-C} = 2.06 \text{ \AA}$ ) or  $\text{Cp}_2\text{Ru}$  ( $\text{Ru-C} = 2.20 \text{ \AA}$  [3,20]) cannot, and in the latter  $\text{Cp}_2\text{Mn}$  is forced to enter in the less voluminous low-spin state.

Finally, it is noteworthy that while the best fit was obtained with models in which both the  $\text{C}(\text{Cp})\text{-H}$  and  $\text{C}(\text{Cp})\text{-C}(\text{Me})$  bonds are bent out of the  $\text{C}_5$  plane of the ring away from the metal atom, the estimated standard deviations render the result insignificant: neither a planar model, nor one in which the bonds are bent towards the metal atom by a few degrees can be ruled out.

### Acknowledgements

We are grateful to Dr. M.L.H. Green for the sample of  $(\text{Mecp})_2\text{Mn}$ , to Dr. Johan Ammeter for stimulating discussions, and to the Norwegian Research Council for Science and The Humanities for financial support.

### References

1. E. Gard, A. Haaland, D.P. Novak and R. Seip. *J. Organometal. Chem.*, 88 (1975) 181.
2. A. Almendingen, A. Haaland and T. Motzfeldt, in *Selected Topics in Structure Chemistry*, Universitetsforlaget, Oslo, 1967, p. 105.
3. A. Haaland and J.E. Nilsson, *Acta Chem. Scand.* 22 (1968) 2653.
4. A. Haaland, J. Lusztyk, D.P. Novak, J. Brunvoll and K.B. Starowieyski, *J. Chem. Soc., Chem. Commun.*, (1974) 54.
5. A.K. Hedberg, L. Hedberg and K. Hedberg, *J. Chem. Phys.*, 63 (1975) 1262.
6. A. Almendingen, E. Gard, A. Haaland and J. Brunvoll, *J. Organometal. Chem.*, 107 (1976) 273.
7. L. Hedberg and K. Hedberg, *J. Chem. Phys.*, 53 (1970) 1228.
8. S. Evans, M.L.H. Green, B. Jewitt, A.F. Orchard and C.F. Pygall, *J. Chem. Soc. Faraday Trans. II*, 68 (1972) 1847.

9. S. Evans, M.L.H. Green, B. Jewitt, G.H. King and A.F. Orchard, *J. Chem. Soc. Faraday Trans. II*, 70 (1974) 356.
10. M.E. Schwitzer, R. Wang, M.F. Rettig and A.H. Maki, *J. Amer. Chem. Soc.*, 96 (1974) 7669.
11. J.H. Ammeter, R. Bucher and N. Oswald, *J. Amer. Chem. Soc.*, 96 (1974) 7833.
12. R.B. King, *Organometallic Synthesis, Vol. I*, Academic Press, New York 1965, p. 67.
13. O. Bastiansen, O. Hassel and E. Risberg, *Acta Chem. Scand.*, 9 (1955) 232.
14. B. Andersen, H.M. Seip, T.G. Strand and R. Stølevik, *Acta Chem. Scand.*, 23 (1969) 3224.
15. J. Ammeter, private communication.
16. H.M. Seip, T.G. Strand and R. Stølevik, *Chem. Phys. Lett.*, 3 (1969) 1937.
17. D.W. Clack, *Theoret. Chim. Acta*, 35 (1974) 157.
18. W. Bünder and E. Weiss, *J. Organometal. Chem.*, 92 (1975) 1.
19. A. Haaland, J. Lusztyk, J. Brunvoll and K.B. Starowieyski, *J. Organometal. Chem.*, 85 (1975) 279.
20. G.L. Hardgrove and D.H. Templeton, *Acta Cryst.*, 12 (1959) 28.